Journal of Neurology and Neurological Disorders
Volume 9 | Issue 1
ISSN: 2454-4981

Research Article Open Access

Prion Disease in Tgmhu2me199k Mice Skeletal Muscle: A Marker for Disease Advance and Treatment Assessment?

Kati Frid[1,2], Tsipora Markovits-Pachter[1,2], Areen Usmann[1,2], Orli Binyamin[1,2], and Ruth Gabizon[1,2*]

[1]Department of Neurology, The Agnes Ginges Center for Human Neuro genetics, Hadassah University Medical Center, Jerusalem, Israel

[2]Medical School, The Hebrew University, Jerusalem, Israel

[*]**Corresponding Author:** Ruth Gabizon, Department of Neurology, The Agnes Ginges Center for Human Neuro genetics, Hadassah University Medical Center, Jerusalem, Israel, Tel no: +972 508573744, E-mail: gabizonr@hadassah.org.il

Citation: Kati Frid, Tsipora Markovits-Pachter, Areen Usmann, Orli Binyamin, Ruth Gabizon (2023) Prion Disease in Tgmhu2me199k Mice Skeletal Muscle: A Marker for Disease Advance and Treatment Assessment? J Neurol Neurol Disord 9(1): 103

Received Date: July 28, 2023 **Accepted Date:** August 28, 2023 **Published Date:** August 30, 2023

Abstract

My ositis and PrP accumulation were observed in muscles of diverse prion affected human and animal models. While in transmissible prion diseases, muscles are most likely infected by the corresponding brain prions, in genetic CJD, muscle pathology may result from a spontaneous mechanism related to the individual properties of each mutant PrP. In this work, we looked for muscle abnormalities in TgMHu2ME199K mice, a model of GCJD linked to the E200KPrP mutation, as well as in TgMHu2ME199K mice treated with Granagard, a nano-formulation of pomegranate seed oil shown to delay disease advance in these mice. We show here extensive abnormalities in the muscles of adult (sick) TgMHu2ME199K mice, including the accumulation of aggregated PrP, central localization of nucleus, and infiltrations of fat cells. We also show decreased levels of axonal markers, indicating muscle denervation, as well as a pronounced reduction in the expression of PAX7, the major marker for quiescent satellite stem cells. Contrarily, long term administration of Granagard reduced muscle levels of aggregated PrP, preserved PAX7 expressing stem cells, and improved muscle mitochondrial activity. We conclude that the pathological findings in adult TgMHu2ME199K muscles may result from both reduced central in nervations caused by the brain disease and from local accumulation of aberrantly folded mutant PrP. We propose that muscle biopsies from human carriers of pathogenic PrP mutations may provide diagnostic indicators of disease initiation and advancement and also serve as a system to test the efficacy of diverse treatments.

Keywords: CJD; Muscles; Brain; Neuro degeneration; Granagard; PAX7; Satellite Cells; Prp; Genetic; Myosin

Abbreviations

WT: wild type; Tg: TgMHu2ME199K; transgenic mouse model for E200K genetic prion disease; CJD: Creutzfeldt-Jakob disease; GCJD: Genetic Creutzfeldt-Jakob disease; FCJD: familial Creutzfeldt-Jakob disease; AD: Alzheimer disease; PD: Parkin-

son disease; ALS: Amyotrophic Lateral Sclerosis; BSE: Bovine Spongiform Encephalopathy; CWD: prion disease in deer; 5x-FAD: a mouse model for AD; PrP: prion protein; PrP^{C}: cellular prion protein; PrP^{Sc}: scrapie infected prion protein PrP, prion protein; PK: protein ase kinase; GranaGard: a nano droplet formulation of Pomegranate Seed Oil (Omega 5); EDL: Extensor digitorum longus; ROS: reactive oxygen species

Introduction

Despite enormous efforts of the scientific community, effective treatments that can reverse the damage caused by neurodegenerative diseases are not yet available [1-3]. Indeed, the current concept in this respect is that such treatments may not be feasible due to the poor regeneration levels in nerve cells and the irreversible neurological damage already present in the preclinical stages [4,5]. This is true for most neurodegenerative conditions, such as AD, ALS, PD and CJD [6,7]. Therefore, there is a consensus among scientists that efforts should be made for the development of prophylactic treatments, such that would delay/prevent disease before it is clinically manifested. To establish the point in time in which prophylactic treatments should commence, especially if side effects are expected, it is imperative to develop tests that can diagnose the "go" point from asymptomatic to sick for each of these conditions [8,9].

While tests that would identify such a point in sporadic diseases in the general population are hard to envision and implement, this is not the case for carriers of pathogenic mutations associated with key disease related proteins in neurodegenerative conditions [10]. Since the disease will present at some point in their adult life, it may well be that early markers exist in such subjects in tissues accessible for sampling. This may be true for individuals carrying dominant pathogenic mutations in the PrP protein linked to genetic CJD, the most common human prion disease [11,12]. These subjects are born healthy, then manifest disease signs at middle age or latter which aggravates to inevitable death.

The pathological accumulation of PrP^{Sc}, the aggregated and protease resistant iso form of PrP, occurs mostly in brains [13]. However, aberrant forms of PrP were also found in other organs, most notably in spleen and muscles [14,15]. Indeed, PrP^{Sc} and prion infectivity in spleen appears early after prion infection of mice [16]. In addition PrP^{Sc} and sometimes prion infectivity were found in muscles from BSE infected cattle [17,18], CWD infected deer [19] and scrapie infected sheep [20] as well as in rodents models of such diseases [21-23]. While in transmissible prion disease it may well be that the presence of disease related PrP forms relates to central nerve degeneration, in genetic diseases intrinsic muscle disease may also be caused by the local aberrant PrP, as shown by PrP accumulation and my ositis in muscles from transgenic mouse models associated with inherited forms of CJD [24,25]. Luckily, and as opposed to brain biopsies which cannot be performed on healthy subjects at risk, muscle biopsies are a commonly ordered diagnostic procedure, used by clinicians to evaluate diverse stages of muscle disease, and are mostly safe [26].

In this work, we tested for the presence of age dependent muscle abnormalities in young and adult TgMHu2ME199K mice, a transgenic line mimicking for CJD linked to the E200K PrP mutation [27]. TgMHu2ME199K mice are born healthy and present first signs of disease at 6-7 month of age, then slowly deteriorate to a fatal state of paralysis at 12-14 months of age [28]. We also examined the properties of skeletal muscles of adult TgMHu2ME199K mice treated with Granagard, a nano formulation of pomegranate seed oil [29-31]. Long term administration of Granagard to these mice was shown to delay disease advancement and death significantly without causing side effects by an energy saving and antioxidant mechanism [32-35].

We found that while young and asymptomatic TgMHu2ME199K mice present normal muscle parameters comparable to those observed in wt mice, adult and sick TgMHu2ME199Kmice (12-14 months old), present high numbers of central nuclei[36]representing both cell damage and regeneration attempts, as well as fat cells infiltration [37], PrP aggregates accumulating mostly within necrotic fibers [38], increased levels of glycolytic fast myosin staining in glycolic muscle [39], reduced enervation and most interestingly, reduced levels of PAX7 positive cells, which are quiescent satellite muscle stem cells responsible for muscle maintenance [40]. Muscles from comparable Granagard treated mice also presented high numbers of multiple nucleus cells, but as opposed to

untreated TgMHu2ME199K mice, demonstrated reduced levels of PrP aggregate sand necrotic fibers, as well asPax7 positive cells similar to muscles in wt mice. They also show reduced levels of fast myosin staining, indicating the presence of normal oxidation pathways. These results are comparable to the effect of Granagard in brains, in which Nest in positive brain stem cells and mitochondrial normal activity were maintained during Granagard administration [35,41].We conclude that the assessment of parameters for prion disease before and after Granagard treatment in TgMHu2ME199Kmuscle tissue may predict disease status and the treatment efficacy. It remains to be established whether human muscles biopsies in carriers of PrP mutation can produce similar results with this or other anti-prion treatment.

Materials and Methods

Ethical Statement

All animal experiments were conducted under the guidelines and supervision of the Hebrew University Ethical Committee, which approved the methods employed in this project (Permit Number: MD-19-15854-5).

Administration of Nano-PSO to Tgmhu2me199k Mice

Nano-PSO was administered to designated groups of TgMHu2ME199K mice (female and male) in their drinking water from 3 months to 12-14months old. Concentrated Nano-PSO (16.5 mL) self-emulsion formulation was diluted in 300 mL of water to form a white emulsion with a final concentration of 1.6% oil, as previously described [32,41]. The regular diet of these mice is Telkad by Invigo. All mice were sacrificed at designated time points when required by the experimental protocol. Brains and muscles (Extensor digit orum long us, quadriceps and soleus) of sacrificed mice were processed for pathological and biochemical experiments.

Western Blot Analysis

Brain extracts from wild-type (wt), TgMHu2ME199K and TgMHu2ME199K treated mice at different time points (3 months old young mice and 12-14 months old adult and treated mice) were homogenized at 10% (W/V) in 10mMTriseHCl, pH 7.4, and0.3 M sucrose. Protein levels were measured by pierce BCA protein assay kit (Thermo Fisher Scientific) and then normalized to 250μg proteins in each sample for PrP detection. For Protein ase K (PK) digestions, samples extracted with 2% sarcosyl on ice were incubated with or without PK (final PK concentrations, 5 μg/mL or 40 μg/mL) for 30 minutes at 37°C. For pellet and supernatants samples, normalized brain homogenates were ultracentrifugation at 100000 g for 1 hour and subsequently pellets were separated from supernatants. Next, all samples were boiled in the presence of SDS, subjected to SDS PAGE and transferred to nitrocellulose membrane for1 hour, 300mA. For α-PrP pAb RTC [42] and HRP α- βactin (ab49900, Abcam) membranes were blocked with 3% milk. The membranes were probed overnight at 4 °C with the primary antibodies (RTC 1:10 0 0, βactin 1:10,0 0 0), and developed with α-rabbit horse radish per oxidase (Jackson Immune Research Laboratories, Inc) at a dilution of 1:10000. Protein signals were obtained using an enhanced chemilum in escent western blotting detection method. Immunore active bands were analyzed using the Image J software.

Pathological Examinations and Immuno cytochemistry

Histological evaluations were performed on paraffin-embedded sections of brain samples from wild-type (wt), TgMHu2ME199K and TgMHu2ME199K treated mice at 3 or 12-14 months of age Serial sections of 4 μm paraffin embedded were prepared for immune histochemical and hematoxylin & eosin (H&E) staining. For immune histochemical staining the sections were boiled in citrate- buffer for 40 minutes before blocking (1h, 5% BSA, 3% NGS, 0.1% Triton- X100), then were treated with different antibodies rabbit α-PrP pAb RTC [42] and rabbit α-Fast Myosin skeletal Heavy chain (#ab91506, abcam), and developed with DAB on the secondary antibody, α-rabbit horse radish per oxidase (Jackson Immune Research Laboratories, Inc).

Immunofluorescence Studies

Histologic evaluations were performed on 4 μm paraffin embedded brain sections. Sections were treated by 0.25% Tritone- X100 for 5 minutes and thereafter boiled in citrate- buffer for 40 minutes before blocking (1h, 5% BSA, 3% NGS, 0.1% Triton- X100). Sections were stained for immune fluorescence with an array of designated antibodies. The antibodies that were used rat α- MBP (#MAB386, millipore),rabbit α-NF-M(#AB1987,chemicon),mouse α- PAX7 (#SC-81648, santa-cruz bio technology), mouse α- My OD (#SPM427, bio test),and rabbit α-PrP pAb RTC[42]. Secondary antibodies (α-rabbit or α-mouse) coupled to Alexa Fluor 488 and 568 were used (Abcam). Nuclei were labeled with Dapi (#4083, cell signaling). Confocal analysis was performed with Nikon A1R Confocal Laser Microscope System using the NIS-Elements C control software.

Statistical Studies

The statistical significance between the studied groups versus the wt group for immunoblot was calculated according to Student's 2-tailed *t* test. Quantification of immunofluorescence or immunohistochemistry was done using ImageJ by measuring the positive stain and analyzed the difference between the experimental groups using 1-way analysis of variance (ANOVA) for the results of multiple groups and the Tukey's post hoc test using IBM SPSS Statistics V.23. The data for the clinical score graph is presented as average ±standard error.

Results

My opathy in Muscle Tissue of Tgmhu2me199k Mice

Samples of skeletal muscle from young (3 months old) TgMHu2ME199Kmice as well as from wt mice were stained with H&E (figure 1A), while samples from adult(12-14 months old) TgMHu2ME199Kand wt mice at the same age were stained either with H&E only (Figure1B. i-iii) or with αPrP pAb RTC(figure1B. iv-vi).While TgMHu2ME199Kmice at 3 months old are still asymptomatic, at 12-14 months old these mice are severely sick and present high levels of brain PrP^{Sc} [27,35]. While figure 1A shows that there is no significant difference between H&E muscle staining of young wt and young TgMHu2ME199K mice, this was not the case for muscle staining in the adult mice (figure 1B). While adult wt mice muscle H&E staining was similar to the young mice tissue, adult TgMHu2ME199K mice muscle tissue presented profound abnormalities such as significant levels of central nuclei, variation in fiber size, necrotic fibers and fat cells infiltration, reminiscence of muscles in other models of prion disease (figure.1B. i-iii) [24]. Figure 1B. iv-vi also shows large numbers of PrP aggregates in adult TgMHu2ME199Kmuscle samples, mostly founded in necrotic fibers. This may suggest that PrP aberrant aggregation is responsible for at least part of the muscle pathology in these mice. Figure1 presents EDL (Extensor digit orum longus) muscles, however parallel results were also obtained for soleus and quadriceps samples (not shown).

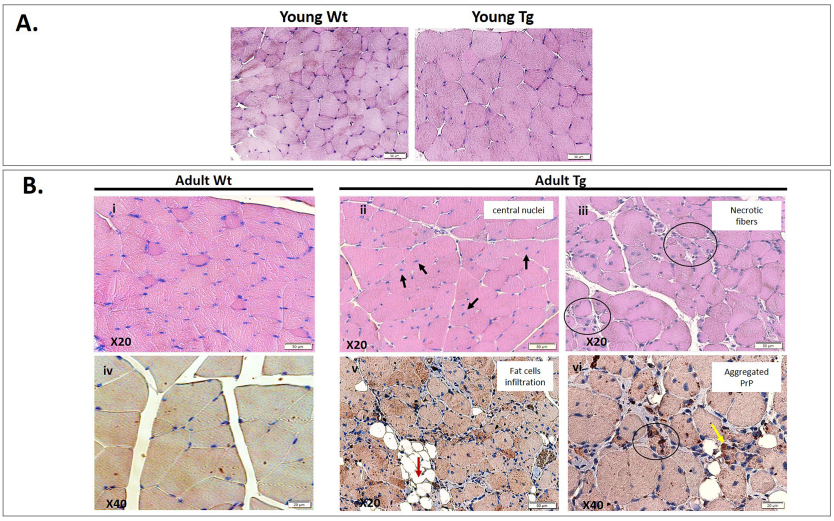

Figure 1: Skeletal muscle pathology in adult TgMHu2ME199K mice. (A) Sections of EDL muscle from young (3 months old) wt and Tg mice were stained with H&E [magnification x20, scale bar 50 μm]. (B) Sections of EDL muscle from adult (12-14 months old) wt and Tg mice were stained with H&E (i-iii) or with RTC an αPrP pAb (iv-vi). Representative images of muscle fibers show adult wt with sub sarcolemmal nuclei stained with H&E and no aggregated PrP forms(brown stain) (i, iv).Muscle sections from adult Tg mice display my opathic features include central nuclei [black arrow] (ii), necrotic fibers [black circle] (iii), infiltration of fat cells [red arrow] (v) and aggregated PrP [yellow arrow] (brown stain) (vi). [magnification x20, scale bar 50 μm; x40, scale bar 20 μm]. Abbreviations: H&E, hematoxylin & eosin; Tg, TgMHu2ME199K; EDL, Extensor digit orum longus.

No PK Resistant Prp Intgmhu2me199k Mice Muscles

Figure 2A shows similar results for PrP staining in adult mice muscle samples by immune fluorescence. Interestingly, this figure also shows that traces of accumulated PrP can be observed in young and asymptomatic TgMHu2ME199K muscles. Low levels of aggregated PrP were also shown in brains of young TgMHu2ME199K mice, already at 10 days of age, and such levels increased with aging and disease aggravation (Binyamin et al., 2017; Frid et al., 2018). However, the conversion of this form of mutant PrP into the PK resistant form, constituting the main hallmark of prion disease [43], occurs mostly at symptomatic stages of disease (Binyamin et al., 2017; Friedman-Levi et al., 2013; Frid et al., 2018). We therefore tested whether this is also true for PrP in muscles of TgMHu2ME199K mice. Figure 2B shows clearly that muscle PrP is not resistant to digestion by high levels of PK such as the ones used for detection of PrP^{Sc}in brains of prion infected subjects [44] as well as in these mice [32]. Lastly, Figure2C shows brain and muscle samples of young (3 months old) and adult (12-14 months old) wt and TgMHu2ME199K mice following digestion with a lower concentration of PK (5μg/ml). As can be seen in the figure, muscle PrP in sick TgMHu2ME199K mice, as opposed to brain PrP, was not resistant to digestion by those PK concentrations, contrarily to what was shown for muscle PrP in other models of prion disease [22,24]. We believe that while the structure of E200KPrP is prone for aggregation [45], it may still require an additional disease related modification to convert into a PK resistant entity [42-46]. Such modification, may occur mostly in the brains of these mice.

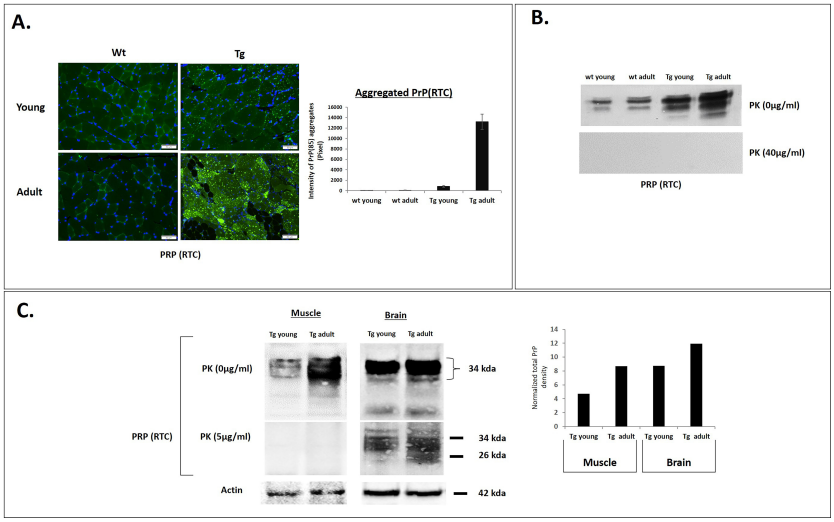

Figure 2: PrP in TgMHu2ME199K mice muscle is not PK resistant.

(A) Immuno fluorescence evaluation of aggregated PrP levels from paraffin embedded quadriceps muscle of young (3 months old) and adult (12-14 months old) wt and Tg mice [magnification x20, scale bar 50 µm]. Quantification was performed by Image J for positive PrP aggregates. (B) muscle extracts from young (3 months old) and adult (12-14 months old) wt and Tg mice were immune blotted with α-PrP pAb RTC before and after PK digestion (40µg/ml). (C) Brain and muscle extracts of adult (12-14 months old) wt and Tg mice were immune blotted with α-PrP pAb RTC in the presence and absence of 5µg/ml PK. All blots were quantified by Image J. In each case, the PrP signal was normalized against the control protein (Actin). Abbreviations: PrP, prion protein; Tg, TgMHu2ME199K; PK, protein ase K.

Denervation in Adult Tgmhu2me199k Mice Muscle

Both demye linating neuropathy and axonal loss are features of neurode generation [47]. To examine if axonal loss by itself can explain muscle degeneration in prion disease, we analyzed the levels of axonal components in muscles of adult TgMHu2ME199K mice as compared to adult wt mice muscles. Skeletal quadriceps muscle samples from adult wt andTgMHu2ME199K mice were immune stained for MBP (myelin basic protein) and NF-M (neuro filament marker), both components of axons [48]. Figure 3A shows NF-M positive axons wrapped with MBP positive myelin fibers in both wt and TgMHu2ME199Kmuscle tissue. As compared to wt mice muscle tissue, adult TgMHu2ME199Kmice samples demonstrate severe denervation that may result from the brain disease. The data was quantified by t-test analysis of stain intensity of an array of such pictures. (NF-M ***p<0.001; MBP ***p<0.001). Next, and to determine whether aggregated PrP in muscles is at least in part of axonal origin, we co-stained adult TgMHu2ME199K mice skeletal muscles with antibodies against MBP and PrP (Figure 3B). Indeed, no co localization was observed between PrP aggregates and the axonal marker, consistent with results in figure 1 indicating PrP aggregates are found in necrotic muscle fibers. These results indicate that aggregation of PrP in TgMHu2ME199K muscles is mostly a local event probably related to the biochemical properties of mutant PrP. The fact that muscle PrP does not convert into PK resistant as brain PrP does reinforces such conclusion. However, this does not rule out the possibility that at least part of muscle abnormalities in TgMHu2ME199Kmice also result from the denervation associated with the central prion disease.

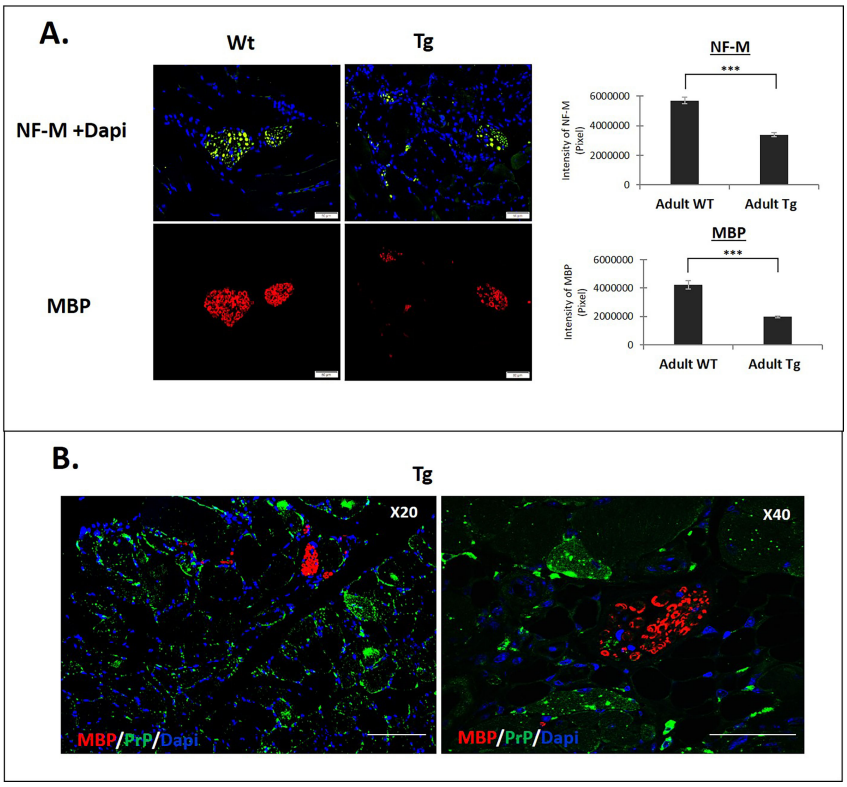

Figure 3: Denervation in adult TgMHu2ME199K mice muscle. (A) Immuno fluorescence evaluation of myelin basic protein (MBP) and neuro filament (NF-M) levels from paraffin embedded quadriceps muscle of adult (12-14 months old) wt and Tg mice [magnification x20, scale bar 50 μm]. Quantification was performed by Image J for positive MBP and NF-M levels in all mice groups. (B) Peripheral nerves of adult Tg mice were Immuno stained against myelin basic protein (MBP) and aggregated PrP protein with α-PrP pAb RTC [magnification x20, scale bar 100 μm magnification x40, scale bar 50 μm]. Abbreviations: Tg, TgMHu2ME199K; PrP, prion protein.

Granagard Effect on Tgmhu2me199k Mice Muscle Abnormalities

We have previously described that long-term administration of Granagard to TgMHu2ME199K mice significantly delayed disease advance by a mechanism involving anti-oxidant and anti-aging hallmarks, tested in the brains of such mice [29, 32,41]. If similar hallmarks could be observed in muscles of TgMHu2ME199K mice treated with Granagard, this will indicate that a muscle biopsy could reflect the results of the treatment efficacy. To this effect, we administrated Granagard to a group of TgMHu2ME199K mice continuously from 3 until 12-14 months and subsequently sacrificed them for biochemical and pathological analysis. Average disease scores for the treated (2.5 at 12-14 months old), as compared to untreated (3.25 at 12-14 months old) mice were tested periodically as described before [32]. Next, we tested whether such long-term administration of Granagard can reduce the presence of aggregated PrP in skeletal muscle. While Granagard administration did not reduce PrP levels in TgMHu2ME199Kbrains [29,32,41], PK sensitive PrP aggregates in muscles (figure2), may relate to the structure of E200K PrP [45] and behave differently. Indeed, as can be seen in figure 4A, immune histochemistry staining of EDL muscles with αPrP pAb RTC demonstrated reduced levels of aggregated PrP forms in the muscles of the treated mice (PrP $^{**}p<0.01$). This reduction of PrP aggregates parallels to the reduction in necrotic fibers following Granagard administration, and may reflect the delay in disease advance of the treated mice as compared to the untreated TgMHu2ME199K mice of the same age [32], indicating reduced PrP and necrotic fibers in TgMHu2ME199K mice muscles may represent reduced disease scores.

Next, we performed H&E staining on samples of wt, treated and untreatedTgMHu2ME199K mice and quantify the number of central nuclei in these groups. Surprisingly, Figure 4B shows a large number of cells presenting central nuclei and even multiple central nuclei in muscles of Granagard treated mice as compared to untreated samples($^{***}p<0.001$). Indeed, while the presence of central nuclei by itself is a pathological event in muscle cells [24], multiple studies have shown that increase in central/multiple nuclei

during treatments may also represent muscle cell regeneration attempts [49,50].

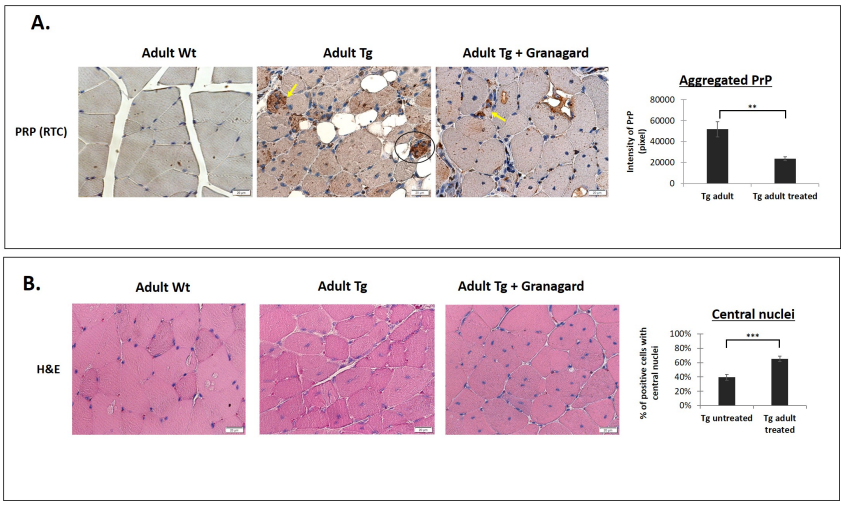

Figure 4: Muscle features of Granagard treated TgMHu2ME199K mice. (A) Paraffin-embedded EDL muscle samples of adult wt, Granagard treated and untreated adult Tg mice were stained for aggregated PrP with α-PrP pAb RTC) yellow arrow((brown stain). [magnification x20, scale bar 50 μm]. (B) Sections of EDL muscle from adult wt, Granagard treated and untreated adult Tg mice were stained with H&E. [magnification x20, scale bar 50 μm]. All quantifications were performed by Image J for positive central nuclei as well as for aggregated PrP in muscle cells. Abbreviations: PrP, prion protein; Tg, TgMHu2ME199K;EDL, Extensor digit orum longus.

Granagard Administration Maintains the Normal Levels of PAX 7 Positive Satellite Cells While Promoting Muscle Proliferation.

We have shown previously that, concomitantly with the advance of the neuro degenerative process, the levels of endogenous brain stem cells in brains of TgMHu2ME199K mice were significantly reduced as compared to wt mice of the same ages [**28,34,**41]. Administration of Granagard preserved neuronal stem cells, as observed by the increased number of Nest in positive cells [**35,41,**51]. Skeletal muscle contains a designated population of adult stem cells, denominated satellite cells, which are responsible for muscle maintenance [52]. Expression of Pax7, a transcription factor, is critical for the normal function of quiescent satellite cells in adult skeletal muscle. When activated to proliferate due to injury or malfunction, satellite cells may down regulate Pax7 and express My **O**D, a my ogenic regulatory factor [53-55].

To investigate whether affected muscles in TgMHu2ME199K mice attempt to regenerate, as opposed to brain cells, we examined the nature of satellite stem cells in muscle tissue of wt, TgMHu2ME199K untreated as compared to those treated with Granagard. Figure 5A shows immune fluorescence staining of positive PAX7 cells (marker of quiescent satellite cells) in EDL muscle samples of wt, treated and untreated TgMHu2ME199K mice. Adult and sick TgMHu2ME199K mice muscle tissue present a significant decrease in the amount of PAX7 positive cells as compared to wt samples, which Granagard treated samples can maintain a significant amount of these cells. Quantification of these data by ANOVA and Benferroni post-hoc test shows significant differences between all tested groups (PAX7 ***$p<0.001$). Concomitantly, EDL muscle slices from wt, treated and untreated TgMHu2ME199K mice were stained with an anti-My OD [56] antibody. Figure 5B shows that while very low levels of My OD stained cells can be observed in wt muscle, significantly levels of My OD are expressed in muscle tissue form both untreated and Granagard treated TgMHu2ME199K mice, indicating the presence of a muscle cell regeneration process [55]. These results are consistent with the notion that regeneration attempts in sick TgMHu2ME199K mice is an active and ongoing process, geared to repair the damage caused to the muscle by the accumulation of aggregated PrP and its oxidation effects [57,33,35]. They also indicate that long term administration of Granagard attenuates the oxidative damage of PrP aggregation in quiescent cells but did not reduce new muscle cells generation.

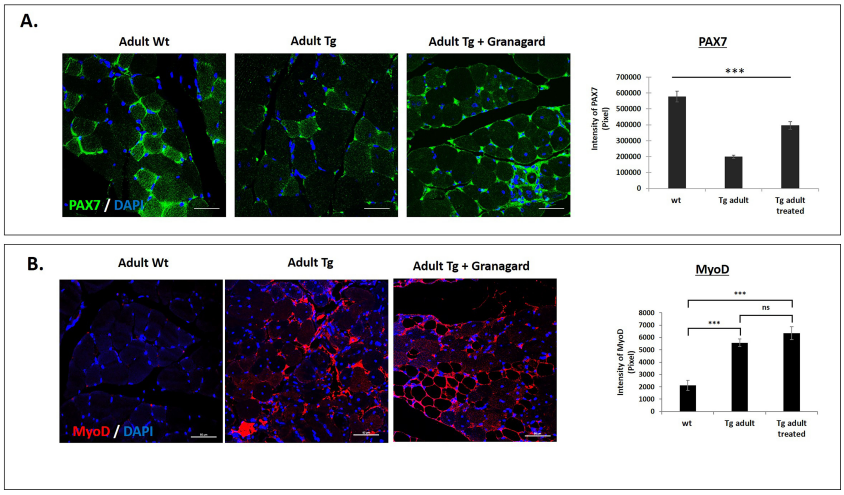

Figure 5: Granagard administration protected satellite muscle cells

(A) Immuno fluorescence evaluation of PAX7 levels (a marker of multi potent satellite cells) of paraffin-embedded EDL muscle from adult wt, Granagard treated and untreated adult Tg mice. (B) Immuno fluorescence evaluation of My OD levels (a marker of proliferating my oblasts) of adult wt, Granagard treated and untreated adult Tg mice. Quantification was performed by Image J for positive PAX7 and My OD levels in treated and untreated mice groups as well as for wt untreated mice [magnification x20, scale bar 50 μm; x40, scale bar 20 μm]. Abbreviations: Tg, TgMHu2ME199K; Granagard, a nano formulation of pomegranate seed oil; EDL, Extensor digitorum longus; H&E, hemat oxylin & eosin.

Granagard Administration Preserves mitochondrial Energy Production Pathways

Oxidative stress and mitochondrial dysfunction are one of the most common features causing damage in muscle diseases [58,59]. We have shown previously that Granagard administration to several mice models of brain disease, as is the case for TgMHu2ME199K for FCJD, 5XFAD for AD as well as for traumatic brain injury model [31,35,60], reduced the levels of ROS and improved mitochondrial activity [33]. Therefore, we next tested the oxidative energy function in muscles of wt, treated and untreated TgMHu2ME199K mice. Slices of EDL muscles of all groups were stained for MyHC (Fast Myosin Skeletal Heavy chain, a marker for glycolic muscle fibers) [61]. Figure 6 displays the results of these experiments, which show higher levels of My HC in cells of untreated TgMHu2ME199K mice when compared to wt or treated TgMHu2ME199K mice (MyHC ***p<0.001byANOVA and Ben ferroni post-hoc test). These results most probably indicate that reduced levels of My HC in Granagard treated mice result from the corrected activity of mitochondrial energy production pathways.

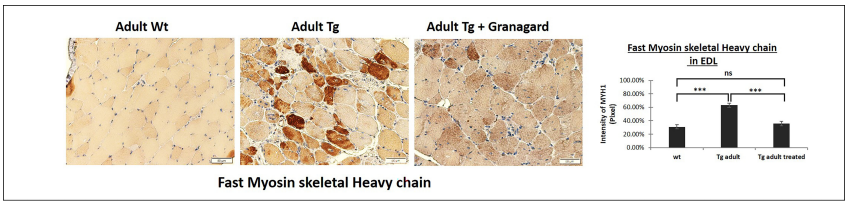

Figure 6: Granagard preserved oxidative energy functions in EDL muscle fibers. Sections of EDL muscle from adult wt, Granagard treated and untreated adult Tg mice were stained with α- Fast Myosin Skeletal Heavy chain (a marker for glycolic muscle fibers). [magnification x20, scale bar 50 μm]. Quantification was performed by Image J for positive glycolic fibers in all mice groups. Abbreviations: Tg, TgMHu2ME199K; Granagard, a nano formulation of pomegranate seed oil; EDL, Extensor digit orum longus.

Discussion

We have shown in this work that skeletal muscles in TgMHu2ME199K mice modeling for genetic CJD linked to the E200K PrP mutation, are significantly damaged at adult age, concomitant with the advance of the neurological prion disease. Similar muscle damage was shown in additional models of genetic as well as prion infected mice, and also in human patients [17,22,24,62]. Mus-

cle damage in these mice is visualized by the presence of central nuclei, necrotic fibers as well as fat cell infiltrations (see figures above). Aggregated muscle PrPinTgMHu2ME199K mice is accumulated inside necrotic fibers, indicating it can play a role in the cell damage, however does not convert into a protease resistant is form, as is the case for TgMHu2ME199Kbrain PrP at the same stages of disease [32]. In addition to the muscle damage caused by the accumulation of mutant PrP, staining with axonal markers such as MBP and NF-M suggests a parallel brain-oriented denervation process, that can by itself promote muscle damage [63,64]. Yet another possibility to explain the apparent muscle damage in TgMHu2ME199K mice, which suffer from a genetic prion disease, is the lack of wt PrP^{C}, the normal PrP iso form, which activity was shown in several studies to be important for muscle maintenance [65-67]. All this together indicates that the mechanism of muscle damage in prion disease, in particular genetic prion disease, is a combination of several factors, all connected to the status of the prion protein and the central fatal disease.

In addition, while brain resident stem cells are mostly non-functional in brains of TgMHu2ME199K mice [41], as is also the case for AD models [68], in muscles of TgMHu2ME199Kmice there is an obvious attempt for regeneration (Figure 5), as seen by the significant levels of My OD positive cells. Granagard treated mice presented lower levels of PAX 7 positive cells as compared to wt mice but still significantly higher than untreated cells, indicating long term administration of Granagard can maintain, at least partially, the activity of quiescent satellite cells. Granagard treated muscles also present high levels of My OD positive cells, demonstrating generation of new cells is active under this treatment.

While TgMHu2ME199K mice treated with Granagard demonstrated a delay in disease score advance [35], it did not result in reduced accumulation of disease related PrP forms in the brain. Interestingly, this was not the case for PrP in muscles, in which accumulation as a PK sensitive aggregated form of PrP decreased significantly during treatment (Figure 4C). In view of these results, and taking into account the different properties of muscle cells from brain cells, we propose that muscle biopsies in mice models may provide a diagnostic indicator of disease advance in prion diseases as well as a parameter of the treatment efficacy [69].

Conclusions

We conclude that the pathological findings in adult TgMHu2ME199K muscles may result both from reduced central enervation caused by the brain disease, as well as from the accumulation of aberrantly folded muscle PrP. It remains to be established whether muscle biopsies from human carriers and patients can also provide diagnostic indicators of disease levels as well as establish the efficacy of diverse treatments.

Funding/Acknowledgment

This project was funded by grants from the Agnes Ginges Center for human genetics and from Granalix Biotechnologies. RG is one of the founders of this company and also its scientific director. None of these institutions is involves in the planning or the dissemination of the experiments results.

References

1. Chopra G, Shabir S, Yousuf S, Kauts S, Bhat SA et al. (2022) Proteinopathies: Deciphering Physiology and Mechanisms to Develop Effective Therapies for Neurodegenerative Diseases. Mol Neurobiol. 59: 7513-40.

2. Mullane K, Williams M (2018) Alzheimer's disease (AD) therapeutics - 2: Beyond amyloid - Re-defining AD and its causality to discover effective therapeutics. Biochem Pharmacol. 158: 376-401.

3. Aguzzi A, Lakkaraju AKK, Frontzek K (2018) Toward Therapy of Human Prion Diseases. Annu Rev Pharmacol Toxicol. 58: 331-51.

4. Kashyap SN, Boyle NR, Roberson ED (2023) Preclinical Interventions in Mouse Models of Frontotemporal Dementia Due to Progranulin Mutations. Neurotherapeutics.

5. Minikel EV, Zhao HT, Le J, O'Moore J, Pitstick R et al. (2020) Prion protein lowering is a disease-modifying therapy across prion disease stages, strains and endpoints. Nucleic Acids Res 48: 10615-31.

6. Manoutcharian K, Perez-Garmendia R, Gevorkian G (2017) Recombinant Antibody Fragments for Neurodegenerative Diseases. Curr Neuropharmacol 15: 779-88.

7. Soo SK, Rudich PD, Traa A, Harris-Gauthier N, Shields HJ et al. (2020) Compounds that extend longevity are protective in neurodegenerative diseases and provide a novel treatment strategy for these devastating disorders. Mech Ageing Dev 190: 111297.

8. Minikel EV, Vallabh SM, Orseth MC, Brandel JP, Haik S et al. (2019) Age at onset in genetic prion disease and the design of preventive clinical trials. Neurology 93: e125-34.

9. Vallabh SM, Minikel EV, Williams VJ, Carlyle BC, McManus AJ et al. (2020) Cerebrospinal fluid and plasma biomarkers in individuals at risk for genetic prion disease. BMC Med 18: 140.

10. Prusiner SB (2013) Biology and genetics of prions causing neurodegeneration. Annu Rev Genet 47: 601-23.

11. Hsiao K, Meiner Z, Kahana E, Cass C, Kahana I et al. (1991) Mutation of the prion protein in Libyan Jews with Creutzfeldt--Jakob disease. N Engl J Med 324: 1091-7.

12. Goldfarb LG, Brown P, Mitrova E, Cervenakova L, Goldin L et al. (1991) Creutzfeldt-Jacob disease associated with the PRNP codon 200Lys mutation: an analysis of 45 families. Eur J Epidemiol 7: 477-86.

13. Bolton DC, McKinley MP, Prusiner SB (1984) Molecular characteristics of the major scrapie prion protein. Biochemistry 23: 5898-906.

14. Glatzel M, Aguzzi A (2000) PrP(C) expression in the peripheral nervous system is a determinant of prion neuroinvasion. J Gen Virol 81: 2813-21.

15. Herzog C, Riviere J, Lescoutra-Etchegaray N, Charbonnier A, Leblanc V et al. (2005) PrPTSE distribution in a primate model of variant, sporadic, and iatrogenic Creutzfeldt-Jakob disease. J Virol 79:14339-45.

16. Lasmezas CI, Cesbron JY, Deslys JP, Demaimay R, Adjou KT et al. (1996) Immune system-dependent and -independent replication of the scrapie agent. J Virol 70: 1292-5.

17. Okada H, Miyazawa K, Fukuda S, Iwamaru Y, Imamura M et al. (2014) The presence of disease-associated prion protein in skeletal muscle of cattle infected with classical bovine spongiform encephalopathy. J Vet Med Sci 76: 103-7.

18. Suardi S, Vimercati C, Casalone C, Gelmetti D, Corona C et al. (2012) Infectivity in skeletal muscle of cattle with atypical bovine spongiform encephalopathy. PLoS One 7: e31449.

19. Daus ML, Breyer J, Wagenfuehr K, Wemheuer WM, Thomzig A et al. (2011) Presence and seeding activity of pathological prion protein (PrP(TSE)) in skeletal muscles of white-tailed deer infected with chronic wasting disease. PLoS One 6: e18345.

20. Garza MC, Monzon M, Marin B, Badiola JJ, Monleon E (2014) Distribution of peripheral PrP(Sc) in sheep with naturally acquired scrapie. PLoS One 9: e97768.

21. Thomzig A, Cardone F, Kruger D, Pocchiari M, Brown P et al. (2006) Pathological prion protein in muscles of hamsters and mice infected with rodent-adapted BSE or vCJD. J Gen Virol 87: 251-4.

22. Bosque PJ, Ryou C, Telling G, Peretz D, Legname G et al. (2002) Prions in skeletal muscle. Proc Natl Acad Sci U S A 99: 3812-7.

23. Westaway D, DeArmond SJ, Cayetano-Canlas J, Groth D, Foster D et al. (1994) Degeneration of skeletal muscle, peripheral nerves, and the central nervous system in transgenic mice overexpressing wild-type prion proteins. Cell 76: 117-29.

24. Chiesa R, Pestronk A, Schmidt RE, Tourtellotte WG, Ghetti B et al. (2001) Primary myopathy and accumulation of PrPSc-like molecules in peripheral tissues of transgenic mice expressing a prion protein insertional mutation. Neurobiol Dis 279-88.

25. Honda H, Mori S, Watanabe A, Sasagasako N, Sadashima S et al. (2021) Abnormal prion protein deposits with high seeding activities in the skeletal muscle, femoral nerve, and scalp of an autopsied case of sporadic Creutzfeldt-Jakob disease. Neuropathology 41: 152-8.

26. Merve A, Schneider U, Kara E, Papadopoulou C, Stenzel W (2022) Muscle biopsy in myositis: What the rheumatologist needs to know. Best Pract Res Clin Rheumatol 36: 101763.

27. Friedman-Levi Y, Meiner Z, Canello T, Frid K, Kovacs GG et al. (2011) Fatal prion disease in a mouse model of genetic E200K Creutzfeldt-Jakob disease. PLoS Pathog 7: e1002350.

28. Fainstein N, Dori D, Frid K, Fritz AT, Shapiro I, Gabizon R et al. (2016) Chronic Progressive Neurodegeneration in a Transgenic Mouse Model of Prion Disease. Front Neurosci 10: 510.

29. Mizrahi M, Friedman-Levi Y, Larush L, Frid K, Binyamin O et al. (2014) Pomegranate seed oil nanoemulsions for the prevention and treatment of neurodegenerative diseases: the case of genetic CJD. Nanomedicine 10: 1353-63.

30. Binyamin O, Larush L, Frid K, Keller G, Friedman-Levi Y et al. (2015) Treatment of a multiple sclerosis animal model by a novel nanodrop formulation of a natural antioxidant. Int J Nanomedicine 10: 7165-74.

31. Binyamin O, Nitzan K, Frid K, Ungar Y, Rosenmann H, Gabizon R (2019) Brain targeting of 9c,11t-Conjugated Linoleic Acid, a natural calpain inhibitor, preserves memory and reduces Abeta and P25 accumulation in 5XFAD mice. Sci Rep 9: 18437.

32. Binyamin O, Keller G, Frid K, Larush L, Magdassi S, Gabizon R (2017) Continues administration of Nano-PSO significantly increased survival of genetic CJD mice. Neurobiol Dis 108: 140-7.

33. Keller G, Binyamin O, Frid K, Saada A, Gabizon R (2019) Mitochondrial dysfunction in preclinical genetic prion disease: A target for preventive treatment? Neurobiol Dis 124: 57-66.

34. Frid K, Binyamin O, Fainstein N, Keller G, Ben-Hur T, Gabizon R (2018) Autologous neural progenitor cell transplantation into newborn mice modeling for E200K genetic prion disease delays disease progression. Neurobiol Aging 65: 192-200.

35. Binyamin O, Frid K, Keller G, Saada A, Gabizon R (2021) Comparing anti-aging hallmark activities of Metformin and Nano-PSO in a mouse model of genetic Creutzfeldt-Jakob Disease. Neurobiol Aging 110: 77-87.

36. Folker ES, Baylies MK (2021) Nuclear positioning in muscle development and disease. Front Physiol 4: 363.

37. Dallaway A, Kite C, Griffen C, Duncan M, Tallis J et al. (2020) Age-related degeneration of the lumbar paravertebral muscles: Systematic review and three-level meta-regression. Exp Gerontol 133: 110856.

38. Cornelio F, Dones I (1984) Muscle fiber degeneration and necrosis in muscular dystrophy and other muscle diseases: cytochemical and immunocytochemical data. Ann Neurol 16: 694-701.

39. Pereyra AS, Lin CT, Sanchez DM, Laskin J, Spangenburg EE et al. (2022) Skeletal muscle undergoes fiber type metabolic switch without myosin heavy chain switch in response to defective fatty acid oxidation. Mol Metab 59: 101456.

40. von Maltzahn J, Jones AE, Parks RJ, Rudnicki MA (2013) Pax7 is critical for the normal function of satellite cells in adult skeletal muscle. Proc Natl Acad Sci USA 110: 16474-9.

41. Frid K, Binyamin O, Usman A, Gabizon R (2020) Delay of gCJD aggravation in sick TgMHu2ME199K mice by combining NPC transplantation and Nano-PSO administration. Neurobiol Aging 95: 231-9.

42. Canello T, Frid K, Gabizon R, Lisa S, Friedler A et al. (2010) Oxidation of Helix-3 methionines precedes the formation of PK resistant PrP. PLoS Pathog 6: e1000977.

43. McKinley MP, Bolton DC, Prusiner SB (1983) A protease-resistant protein is a structural component of the scrapie prion. Cell 35: 57-62.

44. McKinley MP, Meyer RK, Kenaga L, Rahbar F, Cotter R et al. (1991) Scrapie prion rod formation in vitro requires both detergent extraction and limited proteolysis. J Virol 65: 1340-51.

45. van der Kamp MW, Daggett V (2010) Pathogenic mutations in the hydrophobic core of the human prion protein can promote structural instability and misfolding. J Mol Biol 404: 732-48.

46. Wang Y, Shao Q, Hall CK (2016) N-terminal Prion Protein Peptides (PrP(120-144)) Form Parallel In-register beta-Sheets via Multiple Nucleation-dependent Pathways. J Biol Chem 291: 22093-105.

47. Reis R, Hennessy E, Murray C, Griffin EW, Cunningham C (2015) At the centre of neuronal, synaptic and axonal pathology in murine prion disease: degeneration of neuroanatomically linked thalamic and brainstem nuclei. Neuropathol Appl Neurobiol 41: 780-97.

48. Raval-Fernandes S, Rome LH (1998) Role of axonal components during myelination. Microsc Res Tech 41: 379-92.

49. Baghdadi MB, Tajbakhsh S (2018) Regulation and phylogeny of skeletal muscle regeneration. Dev Biol 433: 200-9.

50. Avin KG, Chen NX, Organ JM, Zarse C, O'Neill K et al. (2016) Skeletal Muscle Regeneration and Oxidative Stress Are Altered in Chronic Kidney Disease. PLoS One 11: e0159411.

51. Mazurova Y, Rudolf E, Latr I, Osterreicher J (2006) Proliferation and differentiation of adult endogenous neural stem cells in response to neurodegenerative process within the striatum. Neurodegener Dis 3: 12-8.

52. Dumont NA, Bentzinger CF, Sincennes MC, Rudnicki MA (2015) Satellite Cells and Skeletal Muscle Regeneration. Compr Physiol 5: 1027-59.

53. Zammit PS, Relaix F, Nagata Y, Ruiz AP, Collins CA et al. (2006) Pax7 and myogenic progression in skeletal muscle satellite cells. J Cell Sci 119: 1824-32.

54. Dumont NA, Rudnicki MA (2017) Characterizing Satellite Cells and Myogenic Progenitors During Skeletal Muscle Regeneration. Methods Mol Biol 1560: 179-88.

55. Olguin HC, Yang Z, Tapscott SJ, Olwin BB (2007) Reciprocal inhibition between Pax7 and muscle regulatory factors modulates myogenic cell fate determination. J Cell Biol 177: 769-79.

56. Vicente-Garcia C, Hernandez-Camacho JD, Carvajal JJ (2022) Regulation of myogenic gene expression. Exp Cell Res 419: 113299.

57. Feng B, Wang Z, Liu T, Jin R, Wang S et al. (2014) Methionine oxidation accelerates the aggregation and enhances the neurotoxicity of the D178N variant of the human prion protein. Biochim Biophys Acta 1842: 2345-56.

58. Yin L, Li N, Jia W, Wang N, Liang M et al. (2021) Skeletal muscle atrophy: From mechanisms to treatments. Pharmacol Res 172: 105807.

59. Oba K, Ishikawa J, Tamura Y, Fujita Y, Ito M et al. (2020) Serum growth differentiation factor 15 level is associated with muscle strength and lower extremity function in older patients with cardiometabolic disease. Geriatr Gerontol Int 20: 980-7.

60. Qubty D, Frid K, Har-Even M, Rubovitch V, Gabizon R, Pick CG (2022) Nano-PSO Administration Attenuates Cognitive and Neuronal Deficits Resulting from Traumatic Brain Injury. Molecules 27.

61. Ausoni S, Gorza L, Schiaffino S, Gundersen K, Lomo T (1990) Expression of myosin heavy chain isoforms in stimulated fast and slow rat muscles. J Neurosci 10: 153-60.

62. Peden AH, Ritchie DL, Head MW, Ironside JW (2006) Detection and localization of PrPSc in the skeletal muscle of patients with variant, iatrogenic, and sporadic forms of Creutzfeldt-Jakob disease. Am J Pathol 168: 927-35.

63. Pigna E, Greco E, Morozzi G, Grottelli S, Rotini A et al. (2017) Denervation does not Induce Muscle Atrophy Through Oxidative Stress. Eur J Transl Myol 27: 6406.

64. Xiang Y, You Z, Huang X, Dai J, Zhang J et al. (2022) Oxidative stress-induced premature senescence and aggravated denervated skeletal muscular atrophy by regulating progerin-p53 interaction. Skelet Muscle 12: 19.

65. Stella R, Massimino ML, Sandri M, Sorgato MC, Bertoli A (2010) Cellular prion protein promotes regeneration of adult muscle tissue. Mol Cell Biol 30: 4864-76.

66. Massimino ML, Peggion C, Loro F, Stella R, Megighian A et al. (2016) Age-dependent neuromuscular impairment in prion pro-

tein knockout mice. Muscle Nerve 53: 269-79.

67. Smith JD, Moylan JS, Hardin BJ, Chambers MA, Estus S et al. (2011) Prion protein expression and functional importance in skeletal muscle. Antioxid Redox Signal 15: 2465-75.

68. Fainstein N, Dan-Goor N, Ben-Hur T (2018) Resident brain neural precursor cells develop age-dependent loss of therapeutic functions in Alzheimer's mice. Neurobiol Aging 72: 40-52.

69. Cotta A, Paim JF, Carvalho E, da-Cunha-Junior AL, Navarro MM et al. (2017) The relative frequency of common neuromuscular diagnoses in a reference center. Arq Neuropsiquiatr 75: 789-95.